

## NUMERICAL STUDY ON THE EFFECT OF PERFORATIONS ON THE WAVE DISSIPATION CHARACTERISTICS OF “HORSE-HOOF-SHAPED HOLLOW PILES BREAKWATERS”

Pham Duc Hung<sup>1</sup>, Tran Dinh Hoa<sup>2</sup>

1. Hydraulic Construction Institute

2. Vietnam Academy for Water Resources

**Abstract:** This paper investigates the effect of perforations on the wave dissipation characteristics of Horse-hoof-shaped hollow pile breakwaters (HHPBs) using the Flow3D model. The results indicate that, with varying wave parameters and sea water levels, the wave dissipation coefficient ( $K_I$ ) varies between 0.59 and 0.82, the transmission coefficient ( $K_t$ ) varies between 0.24 and 0.63, and the reflection coefficient ( $K_r$ ) ranges from 0.33 to 0.6, as the perforated ratio on the front side changes from 9.6% to 14%, while the perforated ratio on the rear side remains constant at 11.31%. In particular, the maximum wave energy dissipation (67%) occurs when the front-rear side ratio is 12% - 11.31% and the ratio of water depth to wave height ( $d/H$ ) is 0.8.

**Keywords:** Perforated hollow pile breakwaters, wave energy dissipation, wave transmission, reflection of wave.

### 1. INTRODUCTION

Horse-hoof-shaped Hollow Pile Breakwater (HHPB) is a type of breakwaters for the purpose of reducing waves, limiting coastal erosion and creating alluvial deposits behind the works to restore mangroves.

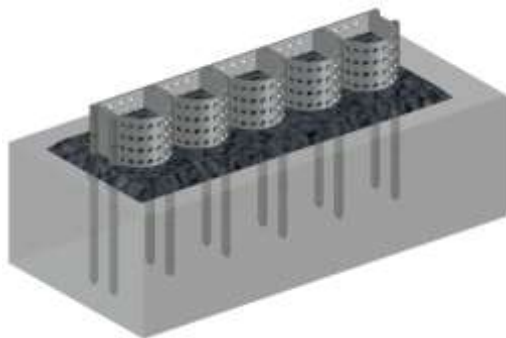


Figure 1: Horse-hoof-shaped Hollow Pile Breakwater [1]

The HHPB (Figure 1) includes 2 components: The front wall (sea side) is in the shape of

semicircular section; the rear wall (field side) is in the shape of box section. Both sides are perforated to absorb and dissipate wave energy. HPBPs are partially embedded in the foundation and supported by special piles to reduce vertical displacement (if necessary). The front and back of the structure are reinforced with a layer of rocks to prevent erosion. Inside the structure is dropped rocks which are used to dissipate wave energy and enhance the overall stability.

Normally, the evaluation of wave dissipation characteristics of breakwaters is carried out using physical models or experimental measurements. However, implementing these physical models can be complex and quite expensive. With the development of numerical models, it is now possible to simulate the hydrodynamic interaction between sea waves and breakwaters quite accurately. In this study, the Flow3D software was used to evaluate the influence of the surface void ratio on the reflection and transmission characteristics of HHPBs.

Receipt Date: October 11<sup>th</sup>, 2022

Review Approval Date: November 15<sup>th</sup>, 2022

Publish Approval Date: December 02<sup>th</sup>, 2022

**2. THEORETICAL MODEL AND SIMULATION SCENARIOS**

**2.1. Theory of Flow3D software**

FLOW3D model has developed by Flow Science INc company which is capable of solving many problems of flow and waves,

Continuity equation:

$$V_F \frac{\partial p}{\partial t} + \frac{\partial}{\partial x}(\rho u A_x) + R \frac{\partial}{\partial x}(\rho v A_y) + \frac{\partial}{\partial z}(\rho w A_z) + \xi \left( \frac{\rho w A_x}{x} \right) = R_{DIF} + R_{SOR} \tag{1}$$

Momentum equations:

$$\begin{aligned} \frac{\partial u}{\partial t} + \frac{1}{V_F} \left\{ u A_x \frac{\partial u}{\partial x} + v A_y R \frac{\partial u}{\partial y} + w A_z \frac{\partial u}{\partial z} \right\} - \xi \frac{A_y v^2}{x V_F} &= -\frac{1}{\rho} \frac{\partial p}{\partial x} + G_x + f_x - b_x - \frac{R_{SOR}}{\rho V_F} (u - u_w - \delta u_s) \\ \frac{\partial v}{\partial t} + \frac{1}{V_F} \left\{ u A_x \frac{\partial v}{\partial x} + v A_y R \frac{\partial v}{\partial y} + w A_z \frac{\partial v}{\partial z} \right\} + \xi \frac{A_y u v}{x V_F} &= -\frac{1}{\rho} \left( R \frac{\partial p}{\partial y} \right) + G_y + f_y - b_y - \frac{R_{SOR}}{\rho V_F} (v - v_w - \delta v_s) \\ \frac{\partial w}{\partial t} + \frac{1}{V_F} \left\{ u A_x \frac{\partial w}{\partial x} + v A_y R \frac{\partial w}{\partial y} + w A_z \frac{\partial w}{\partial z} \right\} &= -\frac{1}{\rho} \frac{\partial p}{\partial z} + G_z + f_z - b_z - \frac{R_{SOR}}{\rho V_F} (w - w_w - \delta w_s) \end{aligned} \tag{2}$$

In these equations:

(Gx, Gy, Gz) are body accelerations,

(fx, fy, fz) are viscous accelerations,

(bx, by, bz) are flow losses in porous media or across porous baffle plates, and the final terms account for the injection of mass at a source represented by a geometry component.

The term  $U_w = (u_w, v_w, w_w)$  is the velocity of the source component, which will generally be nonzero for a mass source at a General Moving Object (GMO).

The term  $U_s = (u_s, v_s, w_s)$  is the velocity of the fluid at the surface of the source relative to the source itself.

$V_F$  = is the fractional volume open to flow

$\rho$  = the fluid density

$R_{DIF}$  = is a turbulent diffusion term

$R_{SOR}$  = is a mass source

$A_x$  = is the fractional open area for flow in the x- direction,  $A_y$  and  $A_z$  are similar area fractions for flow in the y and z directions, respectively.

using the finite volume method to solve the Reynolds Average Navier – Stoke equation [2].

The two main equations of the model are continuity equation and moment equation with the following form:

Besides, FLOW3D can also simulate all waveforms such as: regular waves, random waves, spectral waves... Based on the application of wave theory (Figure 2), choose waveform types suitable for shallow water areas such as: Cnoidal, Solitary, Linear and Stokes wave [3] to evaluate the wave dissipation affection of HHPBs.

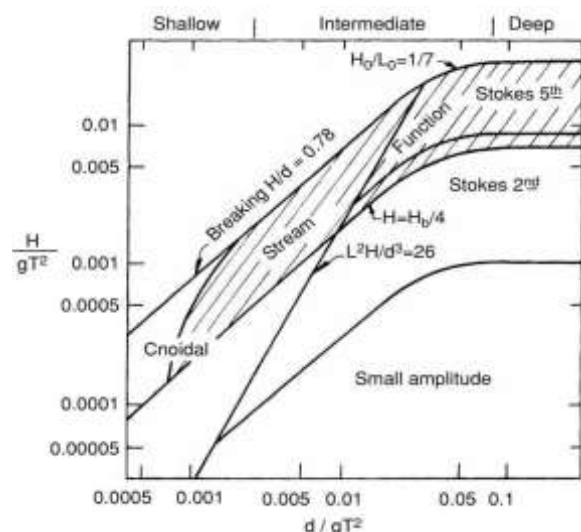


Figure 2: Applicability ranges of various waves [2]

2.2. Set up calculation models and scenarios

The simulation of HHPBs is designed by Autocad-3D software. Then they are imported into Flow3d as .stl form (as shown in Figure 3).

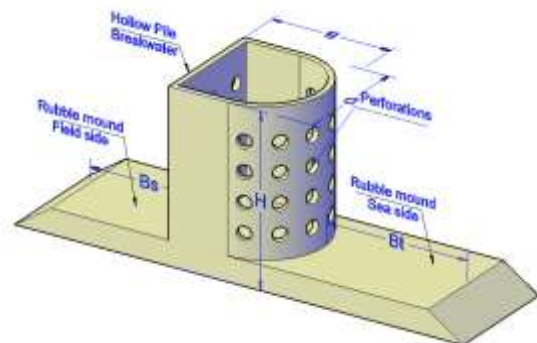


Figure 3: Horse-hoof-shaped hollow pile Breakwater model

The computational domain is simulated at scale of 1:1 with the dimensions of length x width x height. In order to increase the accuracy of the simulation results, the calculation domain is divided into 2 Blocks: Block1 includes the entire simulation domain and HHPBs. Block 2 is the range of the breakwaters (HHPBs). In which, grids of Block 2 were divided with fine mesh size and grids of Blocks 1 were divided with coarser mesh to reduce calculation time. To minimize the effect of reflected waves behind the breakwaters, a 5 m long sponge layer was installed at the end of the model (as shown in Figure 4).



Figure 4: Different mesh blocks for simulation domain

At the left open boundary, the incident wave conditions were imposed. At the right boundary an absorption boundary was adopted to avoid or mitigate the effects of wave reflection. In all other open boundaries, symmetry conditions were defined (as shown in Figure 5). The type of incident wave was defined according to the wave height ( $H_i$ ), period ( $T_p$ ), water depth ( $d$ ) and wavelength ( $L$ ) for the case of cnoidal waves. As initial conditions, wave height ( $H_i$ ), period ( $T$ ), water

depth ( $d$ ) and wavelength ( $L$ ) were defined for the case of stokes waves. As initial conditions, a fluid region was considered along with simulated channel. The fluid used in the simulations was water at 20°C with null salinity.

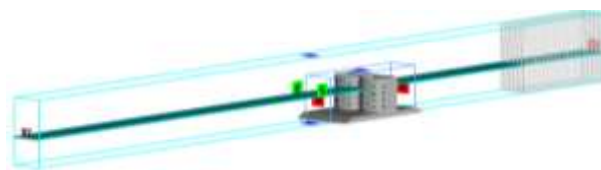


Figure 5: Setup boundary conditions

Validation of simulation model:

For two- or three-dimensional hydraulic problems, the accuracy of the results and the simulation time depends on the size and the number of the cubic cells. It is important to minimize the total number of cells, but at the same time it is necessary to consider a sufficiently high spatial resolution to be able to simulate all the relevant flow patterns and all the details of the geometry. The research teams simulated for 4 different mesh sizes to evaluate the accuracy of the results in order to choose the right mesh size. Specifically, with the mesh size in the case of 0.16 m, the simulation results are different from 5% to 6% compared to the 0.1 m and 0.08 m mesh sizes. With mesh sizes smaller than 0.10 m and 0.08 m, the results are not significantly different (from 1% to 2%). In order to save computer resources as well as reduce calculation time, the mesh size for Block1 was chosen as 0.1m, the mesh size for Block2 was 0.05 m (as shown in Figure 6).

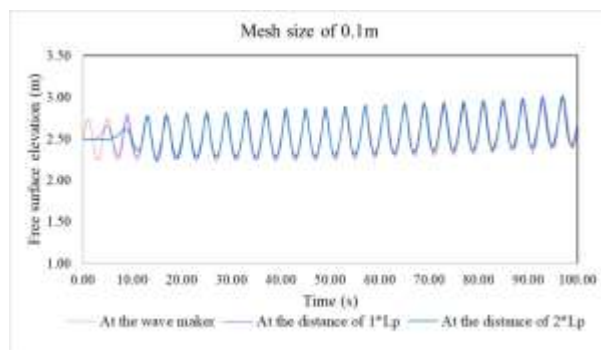


Figure 6: Validation of mesh sizes

Base on the hydrological conditions of the typical area (Mekong Delta). The selected simulation scenarios are defined as Table 1:

**Table 1: Simulated scenarios**

No	Parameters	Values
a	Wave parameters	
1	Wave height, $H_s$ (m)	0.5; 1.0; 1.5
2	Wave period, $T_p$ (s)	4.7 -:- 7.8
3	Relative water depth, $d/H$ (m)	0.6; 0.8; 1.0
b	Structural parameters	
1	Diameter of front surface, $D$ (m)	2.5
2	Width, $B$ (m)	2.5
3	Hight $H$ (m)	3.5
4	Porosity of the front and rear surface, $e\%$	0%-0% 9.6%-11.31% 12%-11.31% 14.4%-11.31%
5	Rubble mound foundation of thickness, $h_d$ (m)	0.5

### 3. RESULTS AND DISCUSSIONS

#### 3.1. The method of determining the wave interaction characteristic coefficients

The 3 probes  $W_1, W_2, W_3$  are arranged to determine the reflected wave followed by the theory of Mansard and Funke (1980) [3], the  $W_4$  probe was placed on leeside to determine the transmitted wave height (as shown in Figure 7). The distance requirements below must be tested to eliminate abnormal values in the measurement.

$$X_{12} = L_p/10;$$

$$L_p/6 < X_{13} < L_p/3 \text{ and } X_{13} \neq L_p/5 \text{ and } X_{13} \neq 3L_p/10;$$

$$X_{12} \neq n \cdot L_p/2, \text{ where } n=1, 2, \dots;$$

$$X_{13} \neq X_{12}, \text{ where } n=1, 2, \dots;$$

Where:  $L_p$ = wave length,  $X_{12}$  = interval distance between probes 1 and 2,  $X_{13}$  = interval distance between probes 1 and 3.

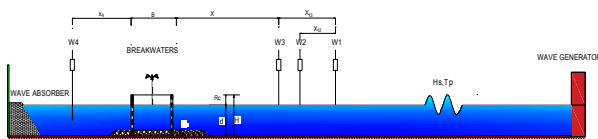


Figure 7: Arrangement of wave probes

The incident wave ( $H_i$ ), reflected wave ( $H_r$ ) and transmitted wave ( $H_t$ ) were analyzed using the wave analysis tool in MIKE zero software. Then, the wave coefficients were calculated following these formulas below:

$$\text{Reflection coefficient: } K_r = \frac{H_r}{H_i} \quad (3)$$

$$\text{Transmission coefficient: } K_t = \frac{H_t}{H_i} \quad (4)$$

$$\text{Loss coefficient: } K_l = \sqrt{1 - K_r^2 - K_t^2} \quad (5)$$

#### 3.2. Effects of surface perforation ratios on the wave attenuation of the PPHBs

##### 3.2.1. Effect of perforations on wave reflection characteristic

Under the same conditions of water depth and wave parameters, increasing the pore surface area of the HHPB leads to a decrease in the reflection coefficient in the simulated scenarios. The maximum value of  $K_r$  is calculated as 1 in the case of non-perforated breakwaters. At this water depth, the minimum calculated value of  $K_r$  is 0.398 when the porosity is between 14.4% and 11.31% (as shown in Figure 8).

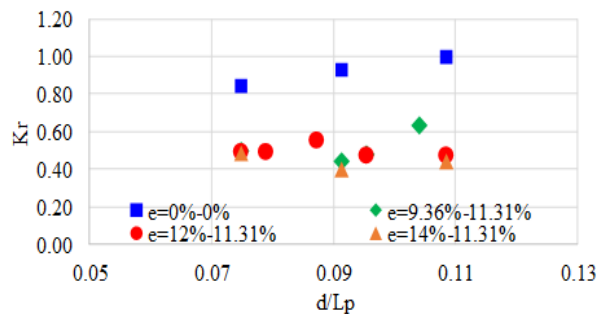


Figure 8: Effect of perforations on  $K_r$  ( $d/H=0.6$ )

At a water depth of 2.8 m ( $d/H=0.8$ ) (as shown in Figure 9), the maximum value of  $K_r$  is 0.82 in the case of non-perforated HHPBs. The HHPBs with a porosity range of 14.4%-11.31% have the smallest value of  $K_r$  at 0.474. For the porosity ranges of 9.6%-11.31% and 12%-11.31%, the calculated values of  $K_r$  are smaller than that of non-perforated breakwaters but bigger than that of HHPBs with  $e=(14.4\%-11.31\%)$ . The range of wave reflection ( $K_r$ ) is from 0.5 to 0.7.

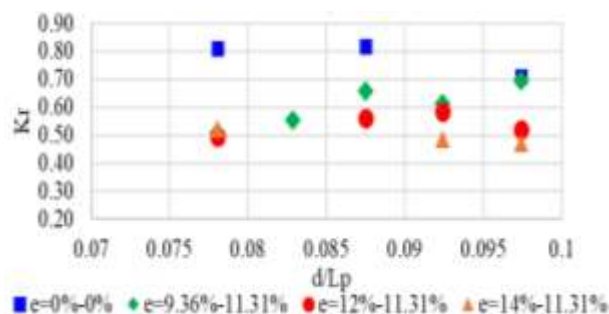


Figure 9: Effect of perforations on  $K_r$  ( $d/H=0.8$ )

When the water level is equal to the height of the structure's top ( $d/H=1$ ) and  $d=3.5$ m, the trend is similar. This means that the reflection coefficient decreases when the surface porosity increases. The case of non-perforated members has the highest reflection coefficient  $K_r$ , ranging from 0.487 to 0.83 (as shown in Figure 10). The minimum value of the wave reflection coefficient varies from 0.32 to 0.5 when the percentage of pore surface area is between 14.4% and 11.31%.

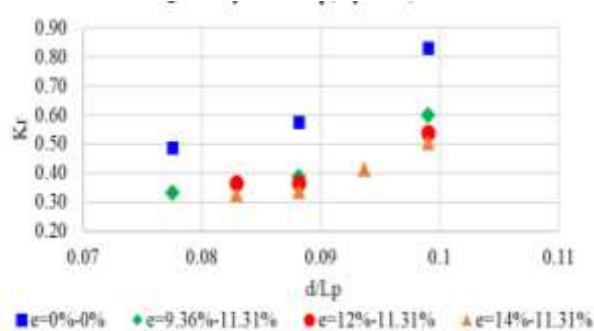


Figure 10: Effect of perforations on  $K_r$  ( $d/H=1.0$ )

### 3.2.2. Effect of perforations on wave transmission characteristic

In general, as the surface void ratio of the member increases, the wave propagation coefficient tends to increase.

For non-perforated HHPBs, at a water depth of  $d=2.1$ m, almost no waves are transmitted with the simulated wave parameters, so the wave transmission coefficient ( $K_t$ ) is close to 0.

For surface-perforated HHPBs, under the simulated wave parameter scenarios, at a water depth of  $d=2.1$ m, Figure 11 shows that the minimum value of  $K_t$  is 0.334 in the case of  $e=(9.6\%-11.31\%)$ , and the maximum value of  $K_t$  is 0.56 in the case of  $e=14.4\%-11.31\%$ .

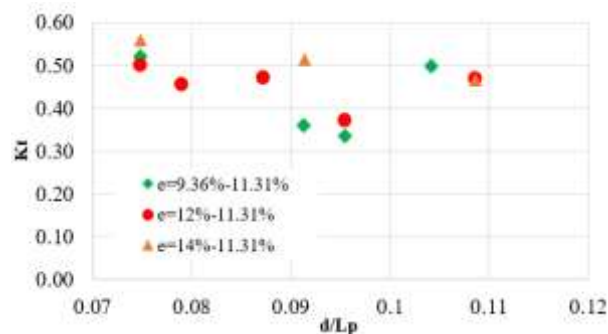


Figure 11: Effect of perforations on  $K_t$  ( $d/H=0.6$ )

As the water depth increases to the ratio of  $d/H$  equals 0.8, the wave transmission through the breakwater increases as the surface pore area ratio increases. The wave transmission coefficient through the perforated HHPBs with  $e=14.4\%-11.31\%$  ranges from 0.42 to 0.52,

while  $K_t$  is from 0.31 to 0.43 when  $e=12\%-11.31\%$ , as shown in Figure 12.

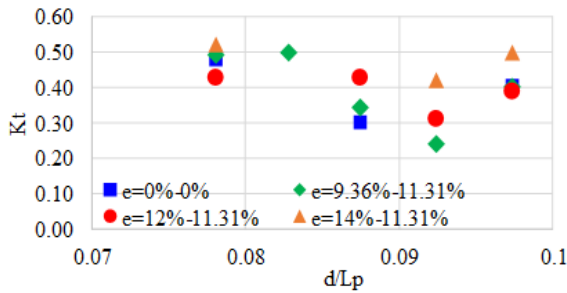


Figure 12: Effect of perforations on  $K_t$  ( $d/H=0.8$ )

In the case of no freeboard ( $R_c = 0$ ), where the hollow piles are completely submerged, the wave propagation characteristics are relatively the same for both perforated and non-perforated breakwaters. The wave transmission coefficient is in the range of  $K_t$  from 0.42 to 0.63, as shown in Figure 13. This can be explained by the fact that when the water level is equal to the crest height, the entire structure is flooded, and the volume of the wave dissipation chamber is no longer available. The incident wave energy is dissipated mainly due to friction with the structures, so  $K_t$  is less affected by perforations but greatly influenced by the width in the

direction of wave propagation. For HHPBs with the same crest width, the waves moving through structures are nearly similar.

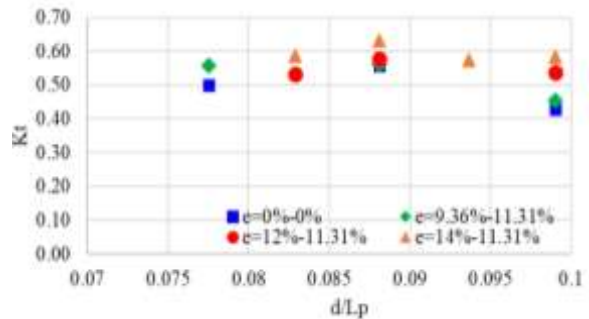


Figure 13: Effect of perforations on  $K_t$  ( $d/H=1.0$ )

### 3.2.3. Effect of perforations on wave dissipation characteristic

Figure 14 illustrates the simulation of the interaction between waves and HHPBs. Based on the calculation results of reflected and transmitted waves, it can be observed that the dissipation coefficient ( $K_I$ ) ranges from 0.33 to 0.82. As the number of perforations on the surface of HHPBs increases, the wave energy dissipation tends to decrease.

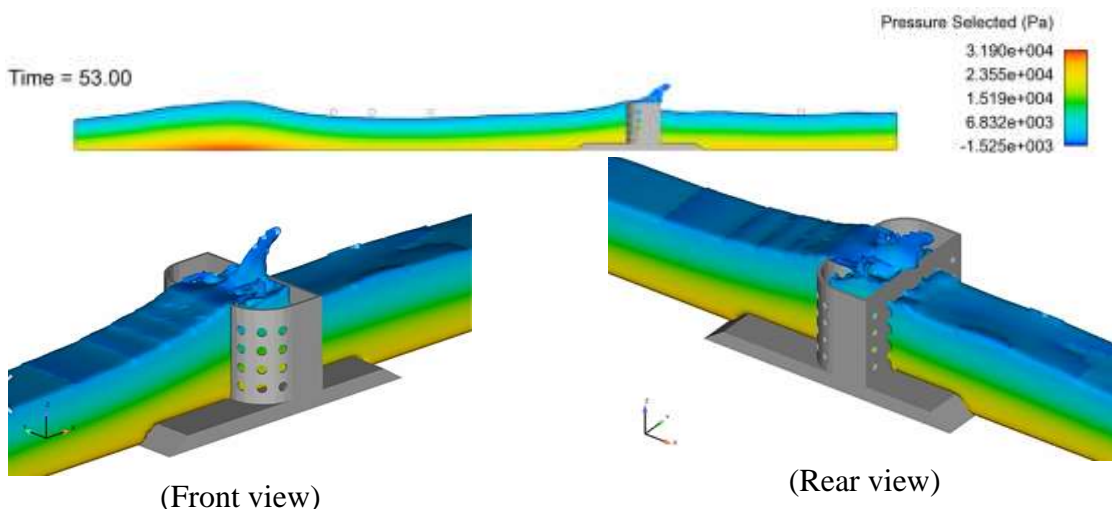


Figure 14: Waves interacting with HHPBs

Under the same conditions of water depth  $d=2.1$  m (as shown in Figure 15), the wave dissipation energy is clearly affected by the

changing of perforations of HHPBs,  $K_{I \min}$  is 0.59 and  $K_{I \max}$  is 0.82 (in case of  $e=(9.6\%-11.31\%)$ ,  $d/H=0.6$ )

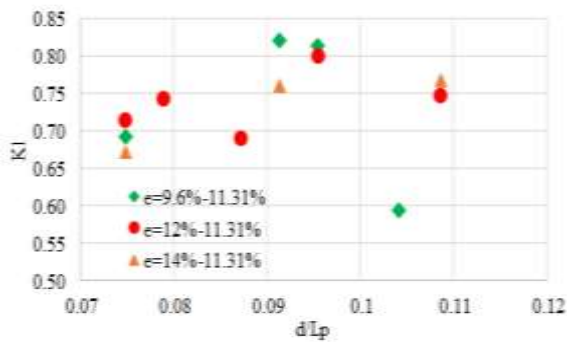


Figure 15: Effect of perforations on  $K_t$  ( $d/H=0.6$ )

At water depths of 2.8 m and 3.5 m, changes in the ratio of pore area on the surface of the HHPBs do not significantly affect the wave energy dissipation capacity. However, there is a clear difference between non-perforated and perforated breakwaters.

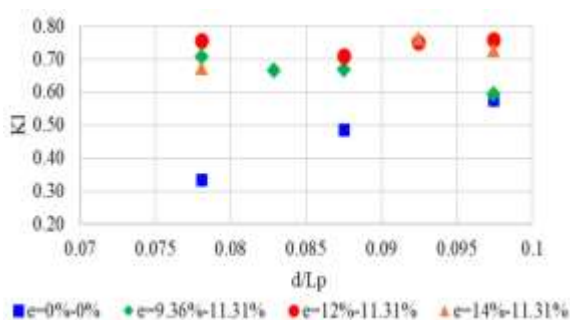


Figure 16: Effect of perforations on  $K_t$  ( $d/H=0.8$ )

The wave energy dissipation coefficients for perforated HHPBs range from 0.6 to 0.8, while those for non-perforated HHPBs range from 0.34 to 0.6, as shown in Figure 16.

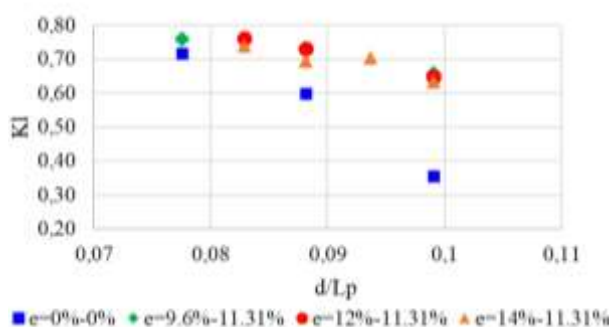


Figure 17: Effect of perforations on  $K_t$  ( $d/H=1.0$ )

In terms of the ratio of incident wave energy distribution, it is evident that for non-perforated structures, the incident wave energy is mostly reflected from 30% to 90%, with the transmitted wave accounting for 0% to 25%, and the lost wave energy being less than 50% of the total incident wave energy.

When the structures are perforated with a certain ratio, the incident wave energy is absorbed and partially dissipated in the wave-absorbing chamber, resulting in a reduction in reflected wave energy. The larger the pore ratio, the lower the reflection, but the transmitted wave energy also increases.

For HHPBs with a perforation proportion of  $e= (9.6\% -11.31\%)$ , the reflected wave energy accounts for 11%-43% of the incident wave energy, while the attenuated and transmitted energy account for 35% to 64% and 10% to 31%, respectively.

In the case of HHPBs with  $e= (12\%-11.31\%)$ , the incident wave energy is distributed as follows: 13%-34% for reflected wave energy, 42%-67% for lost energy, and 10%-33% for transmitted wave energy (refer to Figure 18).

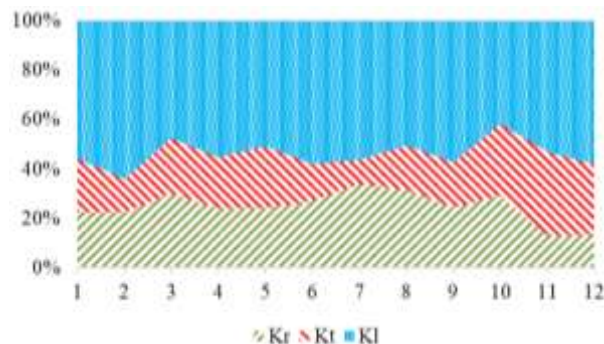


Figure 18: Wave energy distribution in case of  $e= (12\%-11.31\%)$

At a perforation proportion of  $e= (14.4\% -11.31\%)$ , approximately 11% to 28% of the total incident wave energy is reflected wave energy, 18%-35% is transmitted wave energy, and energy loss accounts for 40%-60% of the total incident wave energy.

From all simulated pore ratios, it can be observed that the Horse-hoof-shaped hollow pile Breakwater with a front and rear surface

perforation ratio of  $e=$  (12%-11.31%) exhibits the best wave energy dissipation.

#### 4. CONCLUSIONS

The simulation results of the interaction between waves and structures, with wave boundary conditions of the western sea of the Mekong Delta, indicate that the pore ratio on the surface of the HHPBs has a significant impact on the wave dissipation capacity. The dissipation coefficient ( $K_I$ ) changes from 0.59 to 0.82, the reflection coefficient ( $K_r$ ) ranges from 0.33 to 0.6, and the wave transmission coefficient ( $K_t$ ) varies from 0.24 to 0.63, with variations in the percentage of perforations on the front surface from 9.6% to 14%, and on the

rear surface being 11.31%.

In particular, the maximum wave energy dissipation (approximately 67%) is observed when the front-back surface perforation ratio ( $e$ ) is 12% - 11.31%,  $B=2.5$  m, and  $d/H = 0.8$ .

To further improve this technology, additional studies are required to evaluate other factors that affect the wave attenuation of HHPBs, such as the width of the crest ( $B$ ), the thickness of the rubble mound ( $h_d$ ), the height and size of rocks inside breakwaters, and the pressure acting on HHPBs. Additionally, physical wave flume experiments should be performed to verify the numerical model results and develop additional scenarios.

#### REFERENCES

- [1] Pham Duc Hung, Tran Dinh Hoa, Nguyen Ngoc Nam, "Horse-hoof-shaped hollow pile dyke" – a new solution to coastal protection. *Journal Science and Technology Water Resources*, No.69, pp.2-7.2021;
- [2] "https://www.flow3d.com/," FLOW Science, 2020-2021;
- [3] Stoke, G.G, "On the Theory of Oscillatory Wave," *Mathematical and Physical Papers*, vol 1, pp. 314-326, 1847;
- [4] Mansard, E. P. D., and Funke, E. R. (1980). The Measurement of Incident and Reflected Spectra Using a Least Square Method. *Proc. 17th Coastal Eng. Conf.*, Sydney, Australia, vol. 1, pp. 154-172.